INNOVATION FOREVER
Open Access

Innovation Discovery

ISSN 2959-5150 (Online)

Research Article

The Effect of Tau on Dynamics of Kinesin Motor

Ping Xie[1*]

[1]*Laboratory of Soft Matter Physics, Institute of Physics, Chinese Academy of Sciences, Beijing, China*

[*]***Correspondence to: Ping Xie, PhD, Professor,*** *Laboratory of Soft Matter Physics, Institute of Physics, Chinese Academy of Sciences, No. 8, Zhongguancun South Third Street, Haidian District, Beijing, 100190, China; Email:pxie@aphy.iphy.ac.cn*

Abstract

Kinesin-1 is a motor protein that can perform cargo transport in cells by moving processively on microtubules towards the plus end. Tau, which is expressed at high levels in axons of neurons, is a microtubule-associated protein and can diffuse one-dimensionally on microtubules. It has been shown experimentally that tau can affect the motility of the kinesin motor. Here, an analytical theory is presented for the effect of the diffusive tau on the velocity and run length of the kinesin motor. With no or only one adjustable parameter, which depends on the experimental condition, the theoretical results are in good agreement with the available experimental data. It is found that at a large tau/tubulin ratio, tau has a large effect on the run length of the kinesin motor, with the run length depending sensitively on the diffusion constant of tau. This indicates that the kinesin-based axonal transport could be regulated by the variation of either the concentration or diffusion constant of tau, giving an explanation of why tau can diffuse on microtubules.

Keywords: kinesin, processivity, molecular motor, microtubule-associated protein, diffusion constant, axonal transport

Received: August 5, 2024
Revised: December 2, 2024
Accepted: December 19, 2024
Published: January 22, 2025

Citation: Xie P. The Effect of Tau on Dynamics of Kinesin Motor. *Innov Discov*, 2025; 2(1): 6.

1 INTRODUCTION

Kinesin-1 is a typical motor protein that plays critical roles in long-distance transport of cargo in neural cells[1-5]. The kinesin-1 motor contains two identical motor domains (also called heads) that are connected together by a long coiled-coil stalk via their flexible neck linkers (NLs)[1-6]. Using the energy from Adenosine triphosphate (ATP) hydrolysis the kinesin-1 motor can move on microtubules (MTs) towards the plus end with a velocity of 0.5-1μm/s for a long distance (called run length) of about 1μm before dissociating from MTs. The mechanism of the chemomechanical coupling of the kinesin motor and its dynamics has been studied extensively both experimentally and theoretically[7-16].

Tau is microtubule-associated protein (MAP) that is expressed at high levels in axons of neurons[17,18]. It plays important roles in the regulation of the MT dynamics[17-19] and in the regulation of kinesin-mediated transport[20-25]. Thus, changes in tau expression and/or regulation are related to numerous physiological responses and neurodegenerative disorders such as Alzheimer's disease[24-27]. Tau has multiple isoforms. For example, in humans there are six isoforms[28]. It was found that in 3-repeat short isoform (3RS) tau has a larger effect on the inhibition of the run length of the kinesin-1 motor than in 4-repeat long isoform (4RL)[29]. Moreover, the inhibition of the run length is also dependent on the type of the modification on MTs[29]. For example, on MTs stabilized with paclitaxel and on MTs in the absence of GMPCPP and paclitaxel but including the presence of 10% glycerol and 10% DMSO in the buffer, tau has a large effect on the inhibition of the run length. On GMPCPP-stabilized MTs, no inhibition of the run length was observed. However, in any isoform and on MTs with any type of the modification tau only has a slight effect on the velocity of the kinesin-1 motor[23,29]. Interestingly, it was found that tau can be in either static or diffusing state on the MT lattice[30,31]. In different isoforms and on MTs with different modifications tau molecules have different populations in the diffusing state relative to those in the static state[31]. In the diffusive state, tau can make one-dimensional diffusion

on the MT lattice with a large diffusion constant on the order of 0.1μm^2/s[30,31]. The effects of tau on the velocity of the kinesin-mediated long-distance axonal transport of cargo and the motion of the cargo near tau clusters have also been studied numerically[32].

Despite of the extensive studies, the detailed mechanism of tau regulating the motility of the kinesin-1 motor is still illusive. Concretely, what is the underlying mechanism of tau having only a slight effect on the velocity but having a large effect on the run length of the kinesin-1 motor? What is the underlying mechanism of different tau isoforms or different MT modifications having different effects on the run length? How does the diffusion constant of tau affect the motility of the kinesin-1 motor? To address these unclear issues, here we study theoretically the effect of the diffusive tau on the dynamics of the kinesin-1 motor and compare the theoretical results with the published experimental data[29].

2 METHODS

2.1 Model for Kinesin Motor

We first present the model for the chemomechanical coupling of the kinesin motor, as showed schematically in Figure 1[33,34]. The main elements, on the basis of which the model is set up, are summarized in Section S1 (Figure S1). In this work, we focus on kinesin-1 motor under saturating ATP concentrations and no load on the motor. Since during the processive stepping on MT the kinesin-1 motor shows a very small probability of switching between MT filaments in a step[35], for simplicity, we only consider the stepping along one MT filament and neglect the sideward stepping. For the kinesin-1 motor, since the rate of ATP transition to Adenosine diphosphate (ADP), i.e., ATP hydrolysis and Pi release, in the plus-ended or leading head with the NL not in the plus-ended (forward) orientation is much smaller than that in the minus-ended or trailing head with the NL in the plus-ended orientation, for approximation, we neglect the occurrence of ATP transition to ADP in the leading head. The detailed description of the model (Figure 1) is presented in Section S2.

2.2 Model for Tau

We then present the model for the interaction of tau with a MT filament in the presence of kinesin motors. Prior cryo-electron microscopic observations showed that a tau molecule occupies one tubulin[36,37]. Unless otherwise pointed out, throughout we focus on the conditions as used in the experiments of McVicker et al.[29] and Hinrichs et al[30]. To be consistent with their experimental data[30,31], it is proposed that tau can make unbiased diffusion along a MT filament (Sections 4.1 and 4.2 for detailed discussions) and tau has the similar interaction potential with a MT filament to other MAPs that can diffuse along a MT filament (Figure 2)[38]. The characteristic distance of the interaction between tau and a single tubulin is larger than the periodicity of the MT filament (Figure 2A), resulting in the binding energy (E_{tau}) of tau to a tubulin in the MT filament along the filament direction to be smaller than that (E_{tau}+E_{tau0}) along the direction perpendicular to the filament (Figure 2B). This potential form of tau interacting with a MT filament can result in tau to diffuse readily along the filament by overcoming the smaller binding energy (E_{tau}) along the filament direction without dissociation from MT, because the dissociation is required to overcome the larger binding energy (E_{tau}+E_{tau0}) along the direction perpendicular to the filament. This is consistent with the prior experimental data showing that tau can make the one-dimensional diffusion on MT for a long time before dissociation[30].

2.3 Analytical Expressions for Velocity and Run Length of Kinesin Motor

First, consider the dynamics of kinesin-1 motor in the absence of tau. For kinesin-1, since under no load probability P_E (defined in Figure 1) is nearly equal to one[34], for approximation, we neglect the transition from Figure 1C to A. For kinesin-1 at the INT state (Figure 1B), the rate of the large change in the conformation of the MT-bound head along with the reduction of its affinity for the detached ADP-head and its NL docking is much larger than the rate of ATP transition to ADP in the trailing head of Figure 1A[33]. After the reduction of the affinity between the two heads (Figure 1C), the detached head can bind to MT rapidly (with a time~1μs)[39]. In addition, for the kinesin-1, the ADP release from the MT-bound head is a non-rate-limiting step of the ATPase activity[40]. Thus, the time for the transition from Figure 1A to D, namely the dwell time for a forward step, is approximately τ_0=1/$k^{(+)}$, where $k^{(+)}$ is the rate of ATP transition to ADP in the head with the plus-ended NL orientation or in the trailing head. The velocity of the motor can then be approximately written as

$$v_0 = \frac{d}{\tau_0}, \quad (1)$$

where d=8nm is the periodicity of the tubulins on the MT filament. The run length of the motor can be written as

$$L_0 = \frac{v_0}{\varepsilon_0}, \quad (2)$$

where ε_0 is the dissociation rate of the motor from MT. Note that after the reduction of the affinity between the two heads (Figure 1C), the time for the detached head to bind to MT is so short (~1μs) that the occurrence probability of Period I shown in Figure 1F is negligible. As prior studies showed[33], for the case of no load studied here the dissociation of motor occurs mainly during Period I of Figure 1E, when one ADP-head binds to MT with very weak affinity E_{w1} and the other ADP-head is detached, and during the other weak-MT-binding period (called Period II), when one ADP-head binds to MT with weak affinity E_{w2} and the other ADP-head is detached (not shown in Figure 1).

Then, consider the dynamics of the kinesin motor in the

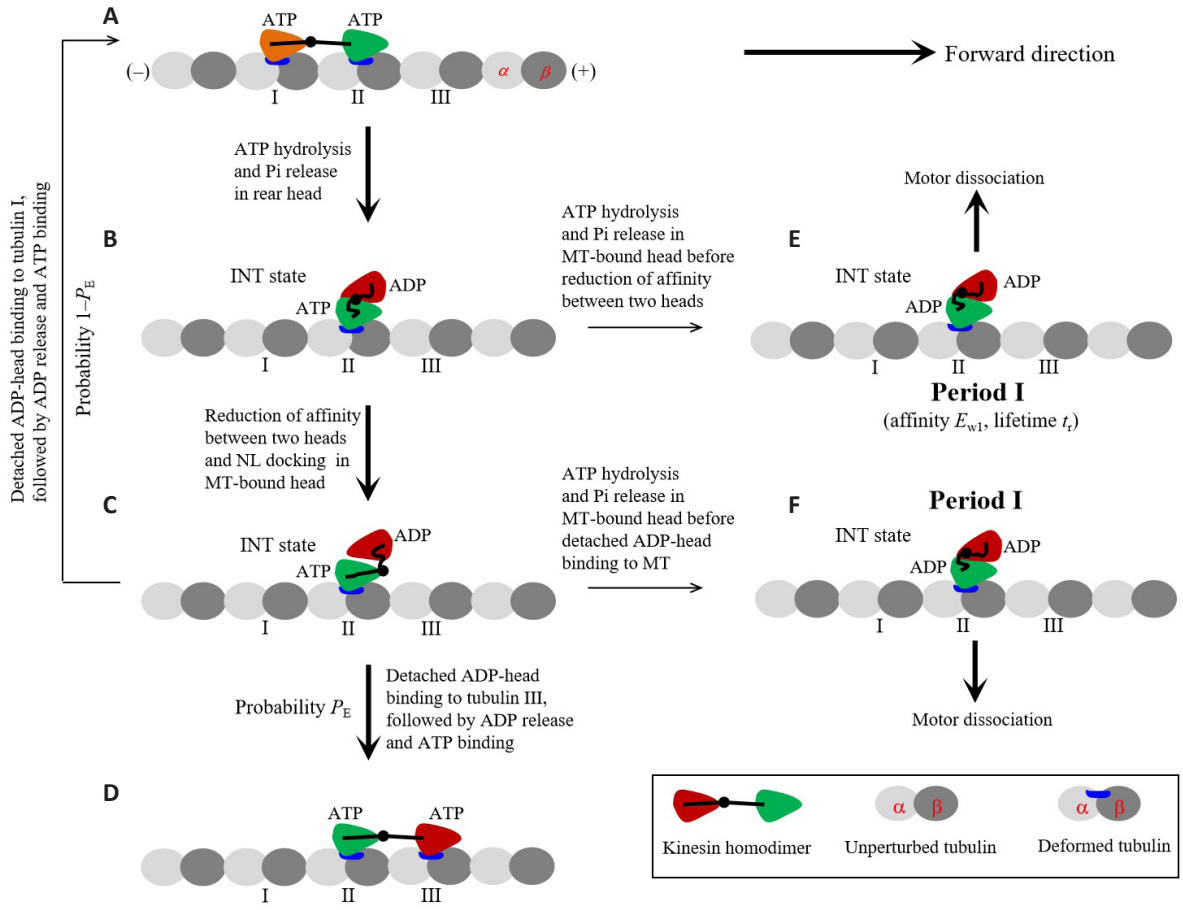

Figure 1. Model for the Chemomechanical Coupling of the Kinesin Motor at Saturating ATP Concentrations. The thickness of an arrow represents the relative magnitude of the probability of the transition between the two states connected by the arrow. A: The trailing and leading heads in ATP state bind strongly to tubulin I and tubulin II, respectively, with the trailing head having a closed nucleotide-binding pocket (NBP), a docked NL and a large change in its conformation relative to the leading head having the open NBP and undocked NL. B: After ATP transition to ADP, the trailing head detaches from the local tubulin I by overcoming the very small affinity E_{w1} and diffuses to the intermediate (INT) position, where it has the high affinity to the MT-bound head. C: At the INT state of the motor, with the NL of the MT-bound ATP-head not driven in the minus-ended orientation, the large change in the conformation of the MT-bound head can take place, closing its NBP, inducing the large decrease of its affinity to the other ADP-head and docking its NL. D:With a probability P_E the detached ADP-head diffuses forward and binds to tubulin III with affinity E_{w2}, followed by ADP release and ATP binding. Correspondingly, with probability 1-P_E the detached ADP-head diffuses backward and binds to tubulin I with affinity E_{w2}, followed by ADP release and ATP binding, with the system returning to (A). Note that the detached ADP-head diffusing backward and binding to tubulin I require undocking the NL and reverse change in the conformation of the ATP-head. E: At the INT state of (B), before the large change in the conformation of the MT-bound ATP-head, ATP transition to ADP can take place occasionally. The motor enters into the state for a short time t_r (called Period I), when one ADP-head binds to the local tubulin II with the very small affinity E_{w1} and the other ADP-head is detached from the MT. During Period I, by overcoming the very small affinity E_{w1} the motor detaches easily from the MT. F: At the INT state of (C), before the detached ADP-head binding to MT, ATP transition to ADP in the MT-bound head can take place, the motor entering into the state of Period I. Note that from (C) the time for the detached ADP-head to bind to MT is so short (~1μs) that the occurrence probability of Period I shown in (F) is negligible. As previous studies showed[33], under no load the detachment of the motor occurs mainly during Period I of (E) and other weak MT-binding period (called Period II) when one ADP-head binds to MT with weak affinity E_{w2} and the other ADP-head is detached from the MT (not shown here).

presence of tau. Throughout, we consider that the number of tau molecules is evidently smaller than that of tubulins, e.g., with the ratio of the former to the latter being smaller than or equal to 1/5, as done in the experiments of McVicker et al[29]. As proposed in Section 2.2 (see also Sections 4.1 and 4.2), tau can make unbiased diffusion along a MT filament, with a large diffusion constant. The relationship between the forward or backward stepping rate and diffusion constant of tau can be written as

$$D = k_{\text{tau}} d^2, \quad (3)$$

where k_{tau} is the forward or backward stepping rate and D is the diffusion constant.

Since tau has a long residence time (about 24.41s) on MT[30], implying a very small dissociation rate of tau from MT and a large binding energy (E_{tau}+E_{tau0}) of tau to MT along the direction perpendicular to the MT filament (Figure 2), it is approximately considered that upon a tau detaching from one MT it can bind to the MT or adjacent MTs rapidly. In other words, it can be considered that at any moment nearly all of tau molecules are bound to MTs[23] although tau molecules detaching from and binding to MTs occur all the time. Considering that the motor number is much smaller than the tau number, it is approximately considered that at one moment the

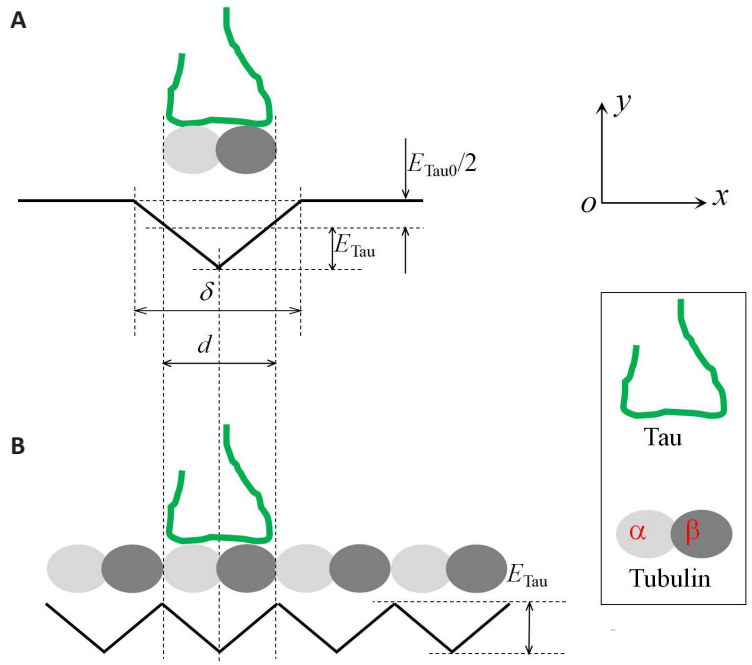

Figure 2. Potentials of Tau Interacting with a Single Tubulin and with a MT Filament. A: The potential of tau interacting with an isolated tubulin. The characteristic distance of the interaction between tau and the tubulin along the *x* direction, which is denoted by δ, is larger than the periodicity of the tubulins on the filament, *d*=8nm. B: The potential of tau interacting with a MT filament. The energy of tau interacting with a tubulin in the filament is E_{tau} along the *x* direction and $E_{tau}+E_{tau0}$ along the *y* direction.

probability of a tubulin on MT filament being occupied by a tau is 1/*R*, where *R* is the ratio of tubulin number to tau number. Consequently, at the INT state of Figure 1C the probability of the front tubulin adjacent to the MT-bound head (called front tubulin) or the rear tubulin adjacent to the MT-bound head (called rear tubulin) being occupied by tau can be approximately written as

$$P_O = \frac{1}{R}. \quad (4)$$

Moreover, the following four situations can occur for the position of tau relative to the MT-bound head of the motor at the INT state of Figure 1C. The first situation is that both the front and rear tubulins are unoccupied by tau. The second situation is that the front tubulin is unoccupied and the rear tubulin is occupied. The third situation is that the front tubulin is occupied and the rear tubulin is unoccupied. The fourth situation is that both the front and rear tubulins are occupied.

Firstly, consider the first and second situations that the front tubulin is unoccupied and the rear tubulin is either occupied or not. The occurrence probability of these situations is (1-P_o). From Figure 1C, the time for the detached head to bind to the front tubulin is so short (~1μs)[39] that during the time ATP transition to ADP in the MT-bound head and a tau diffusion to the front tubulin are negligible. Consequently, for these situations, the probability that Period I cannot occur can be written as

$$P_1 = 1 - P_O. \quad (5)$$

Secondly, consider the third situation that the front tubulin is occupied and the rear tubulin is unoccupied. The occurrence probability of this situation can be calculated by $P_o(1\text{-}P_o)$. Before tau diffusing away from the front tubulin, the detached ADP-head is not allowed to bind to the occupied front tubulin but is allowed to bind to the unoccupied rear tubulin. Since after tau diffusing away from the front tubulin the detached head can bind to the front tubulin instantly, from Figure 1C the time for the detached head to bind to the front tubulin is approximately $1/k_{tau}$. Denoting by E_0 the free energy change associated with the large change in the conformation and NL docking of the head induced by ATP binding, from Figure 1C the time for the detached head to bind to the rear tubulin can be calculated by [34]

$$t_b = t_b^{(0)}\, exp\,(\beta E_0), \quad (6)$$

where $t_b^{(0)}$ is t_b with E_0=0 and $\beta^{-1}=k_BT$ is the Boltzmann constant times the absolute temperature. Thus, from Figure 1C the probability that the detached head can bind to the front tubulin can be written as $k_{tau}/(k_{tau}+1/t_b)$ and the probability that the detached head can bind to the rear tubulin can be written as $1/t_b/(k_{tau}+1/t_b)$ (noting here that during the short time for the detached head to bind to MT, for simplicity, we neglect the small probability of a tau diffusing to the rear tubulin). During the process of the detached head binding to the front tubulin, the probability that Period I cannot occur can be written as $k_{tau}/(k_{tau}+k^{(+)})$. During the process of the detached head binding to the rear tubulin, the probability that Period I cannot occur can be written as $1/t_b/(1/t_b+k^{(+)})$. Consequently, for this situation, the probability that Period I cannot occur can be written as

$$P_2 = P_O(1-P_O)\left(\frac{k_{\text{tau}}}{k_{\text{tau}}+\frac{1}{t_b}}\frac{k_{\text{tau}}}{k_{\text{tau}}+k^{(+)}} + \frac{\frac{1}{t_b}}{k_{\text{tau}}+\frac{1}{t_b}}\frac{\frac{1}{t_b}}{\frac{1}{t_b}+k^{(+)}}\right). \quad (7)$$

Thirdly, consider the fourth situation that both the front and rear tubulins are occupied. The occurrence probability of this situation can be calculated by P_oP_o. From Figure 1C, the time for the detached head to bind to the front tubulin is approximately $1/k_{tau}$ and the time for the detached head to bind to the rear tubulin can be calculated by t_b+1/k_{tau}. Thus, the probability that the detached head can bind to the front tubulin can be approximately calculated by $k_{tau}/[k_{tau}+1/(t_b+1/k_{tau})]$ and the probability that the detached head can bind to the rear tubulin can be approximately calculated by $1/(t_b+1/k_{tau})/[k_{tau}+1/(t_b+1/k_{tau})]$. During the process of the detached head binding to the front tubulin, the probability that Period I cannot occur can be written as $k_{tau}/(k_{tau}+k^{(+)})$. During the process of the detached head binding to the rear tubulin, the probability that Period I cannot occur can be approximately written as $1/(t_b+1/k_{tau})/[1/(t_b+1/k_{tau})+k^{(+)}]$. Consequently, for this situation, the probability that Period I cannot occur can be written as

$$P_3 = P_O P_O \left[\frac{k_{\text{tau}}}{k_{\text{tau}}+\frac{1}{\left(t_b+\frac{1}{k_{\text{tau}}}\right)}} \frac{k_{\text{tau}}}{k_{\text{tau}}+k^{(+)}} + \frac{\frac{1}{\left(t_b+\frac{1}{k_{\text{tau}}}\right)}}{k_{\text{tau}}+\frac{1}{\left(t_b+\frac{1}{k_{\text{tau}}}\right)}} \frac{\frac{1}{\left(t_b+\frac{1}{k_{\text{tau}}}\right)}}{\frac{1}{\left(t_b+\frac{1}{k_{\text{tau}}}\right)}+k^{(+)}} \right]. \quad (8)$$

Therefore, after the reduction of the affinity between the two heads (Figure 1C), the occurrence probability of Period I can be calculated by $P_I^{(\text{tau})} = 1 - P_1 - P_2 - P_3$. With Equations (5), (7) and (8), the above equation for $P_I^{(\text{tau})}$ can be rewritten as

$$\begin{aligned} P_I^{(\text{tau})} &= P_O - P_O(1-P_O)\left(\frac{k_{\text{tau}}}{k_{\text{tau}}+\frac{1}{t_b}} \frac{k_{\text{tau}}}{k_{\text{tau}}+k^{(+)}} + \frac{\frac{1}{t_b}}{k_{\text{tau}}+\frac{1}{t_b}} \frac{\frac{1}{t_b}}{\frac{1}{t_b}+k^{(+)}} \right) \\ &- P_O P_O \left[\frac{k_{\text{tau}}}{k_{\text{tau}}+\frac{1}{\left(t_b+\frac{1}{k_{\text{tau}}}\right)}} \frac{k_{\text{tau}}}{k_{\text{tau}}+k^{(+)}} + \frac{\frac{1}{\left(t_b+\frac{1}{k_{\text{tau}}}\right)}}{k_{\text{tau}}+\frac{1}{\left(t_b+\frac{1}{k_{\text{tau}}}\right)}} \frac{\frac{1}{\left(t_b+\frac{1}{k_{\text{tau}}}\right)}}{\frac{1}{\left(t_b+\frac{1}{k_{\text{tau}}}\right)}+k^{(+)}} \right]. \end{aligned} \quad (9)$$

Since E_{w1} is very small during Period I, it is considered that if Period I occurs the motor can dissociate with a nearly 100% probability, as done before[33,34]. As the presence of tau has a very small effect on the dissociation of the motor during other periods except Period I and the occurrence rate of the INT state of Figure 1C is approximately $k^{(+)}$, the increase in the dissociation rate in the presence of tau relative to that in the absence of tau can be approximately written as $k^{(+)}P_I^{(\text{tau})}$. As a result, in the presence of tau the dissociation rate of the motor can be approximately written as

$$\varepsilon = \varepsilon_0 + k^{(+)}P_I^{(\text{tau})} = \varepsilon_0\left(1+\frac{k^{(+)}P_I^{(\text{tau})}}{\varepsilon_0}\right). \quad (10)$$

After the reduction of the affinity between the two heads (Figure 1C), in the presence of tau the increase in the probability of the detached head binding to the rear tubulin relative to that in the absence of tau can be calculated by

$$\begin{aligned} P_{\text{rear}}^{(\text{tau})} &= P_O(1-P_O)\frac{\frac{1}{t_b}}{k_{\text{tau}}+\frac{1}{t_b}}\frac{\frac{1}{t_b}}{\frac{1}{t_b}+k^{(+)}} \\ &+ P_O P_O \frac{\frac{1}{\left(t_b+\frac{1}{k_{\text{tau}}}\right)}}{k_{\text{tau}}+\frac{1}{\left(t_b+\frac{1}{k_{\text{tau}}}\right)}}\frac{\frac{1}{\left(t_b+\frac{1}{k_{\text{tau}}}\right)}}{\frac{1}{\left(t_b+\frac{1}{k_{\text{tau}}}\right)}+k^{(+)}}. \end{aligned} \quad (11)$$

Thus, in the presence of tau the increase in the dwell time for a forward step relative to that in the absence of tau can be approximately written as $\tau_0 P_{\text{rear}}^{(\text{tau})}$, where $\tau_0=1/k^{(+)}$ is the dwell time for a forward step in the absence of tau, as defined above.

Consequently, in the presence of tau the dwell time for a forward step has the form

$$\tau = \tau_0\left(1+P_{\text{rear}}^{(\text{tau})}\right). \quad (12)$$

In the presence of tau, the velocity of the motor can be calculated by

$$v = \frac{d}{\tau}. \quad (13)$$

With Equations (1) and (12), (13) can be rewritten as

$$\frac{v}{v_0} = \frac{1}{1+P_{\text{rear}}^{(\text{tau})}}. \quad (14)$$

In the presence of tau, the run length of the motor can be calculated by

$$L = \frac{v}{\varepsilon}. \quad (15)$$

With Equations (2), (10) and (14), (15) can be rewritten as

$$\frac{L}{L_0} = \frac{1}{\left(1+P_{\text{rear}}^{(\text{tau})}\right)\left(1+\frac{k^{(+)}P_I^{(\text{tau})}}{\varepsilon_0}\right)}. \quad (16)$$

3 RESULTS

From equations presented in Section 2.3, it is seen that to calculate v/v_0 and L/L_0, values of parameters $k^{(+)}$, E_0, $t_b^{(0)}$ and ε_0 for kinesin, value of parameter D for tau and value of tubulin/tau ratio R are required. As defined above, E_0 is the free energy change associated with the large conformational change and NL docking of the kinesin head induced by ATP binding. $k^{(+)}$ is the rate of ATP transition to ADP in the kinesin head with the plus-ended NL orientation. ε_0 is the dissociation rate of the kinesin motor during its processive stepping on MT in the absence of tau. $t_b^{(0)}$ is the time of the detached ADP-head binding to the rear tubulin in the absence of unoccupied front tubulin for the ideal case of $E_0=0$, which occurs after the reduction of the affinity between the two heads of the motor in the INT state. D is the diffusion constant of tau. R is the ratio of tubulin number to tau number. The values of these parameters are chosen as follows. McVicker et al.[29] measured experimentally that in the absence of tau the velocity of the kinesin motor moving on paclitaxel-stabilized MTs is v_0=0.46μm/s and the run length is L_0=1.31μm. From Equations (1) and (2) and with $\tau_0=1/k^{(+)}$, we obtain $k^{(+)}$=57.5s^{-1}and ε_0=0.35s^{-1}. By comparing the theoretical results with the single molecule optical trapping data on the load dependence of velocity for *Drosophila* kinesin-1 motor in the absence of tau[41], it was determined that $E_0=3.8k_BT$ before[34]. As analyzed before[34], $t_b^{(0)}$=10μs. Thus, in the calculation, we take $k^{(+)}$=57.5s^{-1}, ε_0=0.35s^{-1}, $E_0=3.8k_BT$ and $t_b^{(0)}$=10μs (Table 1).

Table 1. Parameter Values for Kinesin Motor

Parameter	Value	References
$k^{(+)}$	57.5s^{-1}	[29]
ε_0	0.35s^{-1}	[29]
E_0	3.8k_BT	[34]
$t_b^{(0)}$	10μs	[34]

We take diffusion constant D of tau and tubulin/tau ratio R to be variable.

First, we compare our theoretical results with the experimental data of McVicker et al.[29] with tubulin/tau ratio R=5. Using Equation (14) and (16) and with parameter values listed in Table 1, the calculated results of v/v_0 and L/L_0 versus D for R=5 are shown in Figure 3. To see how the theoretical results respond to the variation of the four parameter values, we study the effect of the variation of each parameter value by±10% on the results of v/v_0 and L/L_0 (Figure S2). It is seen that the variation of each parameter value by±10% only has a slight effect on the results (Figure S2). The experimental data of Hinrichs et al.[30] showed that the diffusion constant of tau on paclitaxel-stabilized MTs is D=0.153μm^2/s under the condition with BRB80 buffer (80mM PIPES, 1mM $MgCl_2$, 1mM EGTA, 10mg/ml glucose, pH 6.8). From Figure 3A, it is seen that at D=0.153μm^2/s the theoretical value of v/v_0 is about 0.92, implying that the velocity in the presence of tau is close to that in the absence of tau. This is consistent with the available experimental data showing that tau only has a slight effect on the velocity of the kinesin motor[23,29]. From Figure 3B, it is seen that at D=0.153μm^2/s the theoretical value of L/L_0 is also in agreement with the experimental data (red dot and blue square in Figure 3B) measured by McVicker et al.[29] using paclitaxel-stabilized MTs and under the condition with BRB80 buffer (80mM PIPES, pH 6.9, 1mM EGTA, 2mM $MgSO_4$) which is similar to that of Hinrichs et al.[30]. Since all parameter values are taken from the literature, it is remarkable that with no adjustable parameter, our theoretical results for both the velocity and run length are in agreement with the available experimental data for R=5.

Moreover, from Figure 3A and B it is seen that at D>2μm^2/s, both v/v_0 and L/L_0 approaches 1, giving an explanation of the experimental data of McVicker et al.[29] showing that on GMPCPP-stabilized MTs and MTs stabilized with both paclitaxel and GMPCPP tau has no effect on the inhibition of kinesin motility. This indicates that tau shows a higher diffusivity on GMPCPP-MTs than on paclitaxel-stabilized GDP-MTs, implying that tau has a lower affinity for GMPCPP-MTs than for paclitaxel-stabilized GDP-MTs, which is consistent with available experimental data showing that tau binds weaker to GMPCPP-MTs over GDP-MTs[42,43].

Second, we study the dependence of velocity and run length on D for different values of R. In Figure 4A and B we show the theoretical results of v/v_0 and L/L_0, respectively, versus D for different values of R. From Figure 4A it is seen that even when both R and D are small, tau only has a small effect on the velocity. By contrast, from Figure 4B it is seen that when R is small and D is not large, tau has a sensitive effect on the run length, with L/L_0 increasing significantly with the increase of D. When D is large, L/L_0 becomes saturation to the maximum value of one. These results indicate that in neurons the long-distance kinesin-based axonal transport can be regulated, besides by the variation of the concentration of tau, also by the variation of the diffusion constant of tau, giving an explanation of why tau can diffuse on MTs.

Third, we study the dependence of velocity and run length on tubulin/tau ratio (Figures 5 and 6), comparing with the experimental data of McVicker et al.[29] measured under the condition in the absence of GMPCPP and paclitaxel but including the presence of 10% glycerol and 10% DMSO in the buffer, termed as the condition with glycerol/DMSO. By taking D=0.01μm^2/s, our theoretical results reproduce the experimental data of L/L_0 versus R for 3RS-tau[29] (Figure 5B). The effect of the variation of this value of D on the results of v/v_0 and L/L_0 is shown in Figure S3, from which it is seen that the variation of D by±10% only has a very small effect on the results. By taking D=0.1μm^2/s, our theoretical results are in agreement with the experimental data of L/L_0 versus R for 4RL-tau (Figure 6B)[29]. The effect of the variation of this value of D on the results of v/v_0 and L/L_0 is shown in Figure S4, from which it is seen that the variation of D by±10% also has a very small effect on the results. From Figure 5A and 6A it is seen that in the region of R≥8, v/v_0 is larger than 0.9, indicating that tau has only a slight effect on the velocity, which is also consistent with the prior experimental data[23,29]. In one word, with only one adjustable parameter D, our theoretical results for both the velocity and run length are in agreement with the available experimental data on the dependence of velocity and run length upon tubulin/tau ratio. The determined value of D=0.1μm^2/s for 4RL-tau which is larger than that of D=0.01μm^2/s for 3RS-tau is consistent with the prior experimental data showing that for 4RL-tau a larger fraction of the molecules are in diffusing state than for 3RS-tau[31]. The value of D=0.1μm^2/s for 4RL-tau which is 10-fold larger than that of D=0.01μm^2/s for 3RS-tau implies that under the condition with glycerol/DMSO 4RL-tau has a binding energy E_{tau} (defined in Figure 2A) that is about $\ln(10)k_BT$=2.3k_BT smaller than 3RS-tau. For 3RS-tau, the value of D=0.153μm^2/s under the condition using paclitaxel-stabilized MTs is about 15-fold larger than that of D=0.01μm^2/s under the condition with glycerol/DMSO. This implies that 3RS-tau has a binding energy E_{tau} for paclitaxel-stabilized MTs which is about $\ln(15)k_BT$=2.7k_BT smaller than that for MTs treated with glycerol/DMSO.

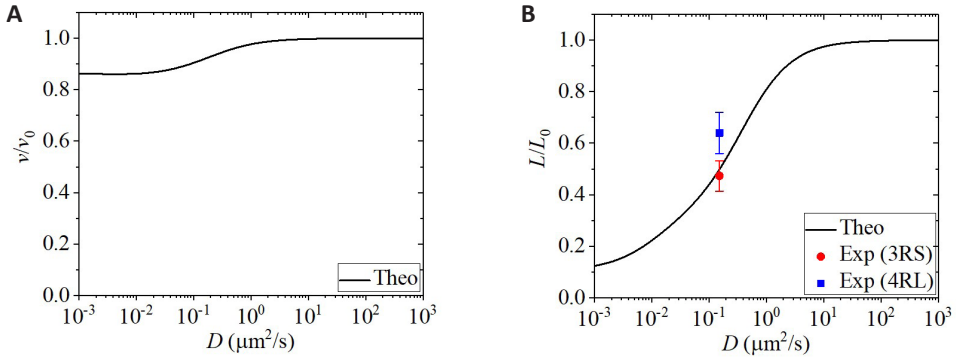

Figure 3. Dependence of the Dynamics of the Kinesin Motor on Diffusion Constant of Tau, *D*, for Fixed Tubulin/Tau Ratio, *R*=5. A: Ratio of velocity of the motor in the presence of tau to that in the absence of tau, v/v_0, versus *D*. B: Ratio of run length of the motor in the presence of tau to that in the absence of tau, L/L_0, versus *D*. The experimental data D=0.153μm²/s is from Hinrichs et al.[30] and the experimental data for L/L_0 are from McVicker et al.[29] measured using paclitaxel-stabilized MTs, with red dot for 3RS-tau and blue square for 4RL-tau.

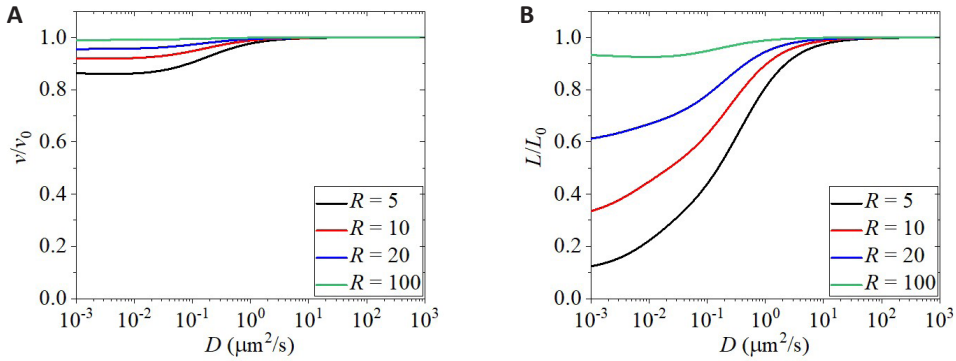

Figure 4. Dependence of the Dynamics of the Kinesin Motor on Diffusion Constant of Tau, *D*, for Different Values of Tubulin/tau Ratio, *R*. A: Ratio of velocity of the motor in the presence of tau to that in the absence of tau, v/v_0, versus *D*. B: Ratio of run length of the motor in the presence of tau to that in the absence of tau, L/L_0, versus *D*.

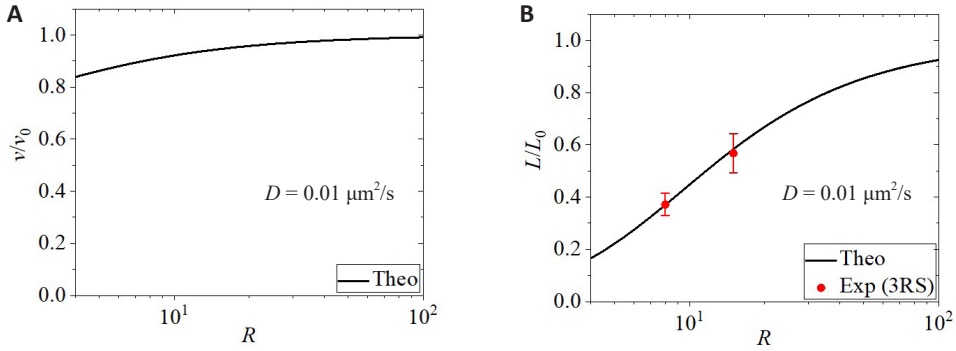

Figure 5. Dependence of the dynamics of the kinesin motor on tubulin/tau ratio, *R*, for fixed diffusion constant of tau, *D*=0.01μm²/s. A: Ratio of velocity of the motor in the presence of tau to that in the absence of tau, v/v_0, versus *R*. B: Ratio of run length of the motor in the presence of tau to that in the absence of tau, L/L_0, versus *R*. Red dots are experimental data from McVicker et al.[29] measured under the condition with glycerol/DMSO for 3RS-tau.

Together, our results (Figures 3-6) indicate that either the variation of the tau concentration or the variation of the diffusion constant of tau can regulate the kinesin motility.

4 DISCUSSION

4.1 Binding of Kinesin Motors to MT Could Alter Tau State

As reviewed recently[44], kinesin motors can induce conformational changes of tubulins while they are stepping on them and these conformational changes appear to propagate along the MT filament to influence other MAPs on the same filament. Specifically, all-atom MD simulation studies showed that the strong interaction between a kinesin head and a tubulin can induce rapidly (on the order of 10 ns) large conformational changes of the tubulin[45]. Experimental studies showed that the binding of kinesin motors can extend the MT lattice along its axis[46,47] and thus can affect the binding of other kinesin motors distant away along the MT[48-50]. Experimental data indicated that the motility of the

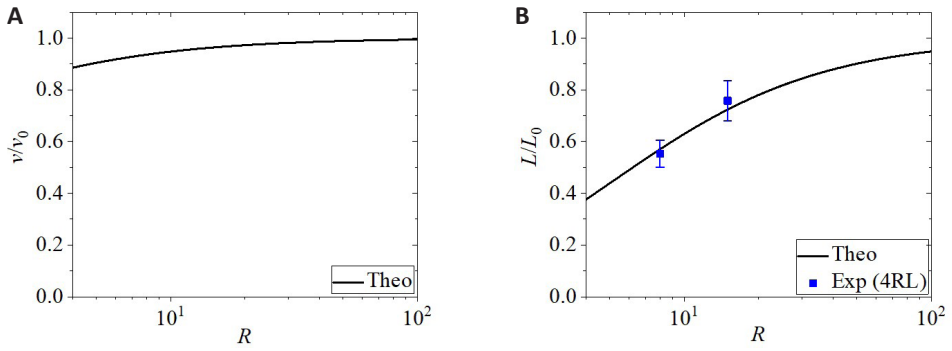

Figure 6. Dependence of the Dynamics of the Kinesin Motor on Tubulin/tau Ratio, *R*, for Fixed Diffusion Constant of Tau, *D*=0.1μm²/s. A: Ratio of velocity of the motor in the presence of tau to that in the absence of tau, v/v_0, versus *R*. B: Ratio of run length of the motor in the presence of tau to that in the absence of tau, L/L_0, versus *R*. Blue squares are experimental data from McVicker et al.[29] measured under the condition with glycerol/DMSO for 4RL-tau.

kinesin-4 motor on MT can be affected by other kinesin motors distant away[51], which was explained theoretically by proposing that the large conformational changes of a tubulin (called tubulin 0) induced by the strong interaction with kinesin can propagate along the MT filament to cause subtle conformational changes of other tubulins and the subtle changes decay exponentially with the distance of the tubulin to tubulin 0[52]. As mentioned in Introduction, the single molecule imaging studies showed that tau can be in both static and diffusive states, which can be altered by subtle changes to the MT architecture[30,31]. This indicates that tau can have multiple states which exist in equilibrium and the states are sensitive to the subtle change of the tubulin conformation. Moreover, recent studies showed that extending the MT lattice can induce the disassembly of the static, interacting tau molecules[53].

Based on these pieces of evidence, it is reasonably argued here that the binding of the kinesin motor to MT can induce the large conformational changes of the local tubulin, which can cause the subtle conformational changes (or extension) of the nearby tubulins, thus inducing tau molecules bound to these tubulins to transition from static to diffusive state and altering the diffusion constant of the diffusive tau. The transition of tau from static to diffusive state and alteration of the diffusion constant of the diffusive tau could arise from the change in the interacting strength between tau and the tubulins, which is induced by the subtle conformational changes of the tubulins. In other words, it is argued here that in the presence of kinesin motors bound to MT filament the nearby tau molecules are in the diffusive state and different modifications of the MT can result in different diffusion constants of the diffusive tau.

4.2 Effect Of Stationary Obstacles on Run Length of Kinesin-1 Motor

Using single-molecule fluorescence and dark-field scattering microscopy, Schneider et al.[54] studied the effect of stationary obstacles (e.g., rigor-binding mutants of kinesin-1) on the dynamics of wild-type kinesin-1 motor. They found that upon encountering a stationary obstacle, the kinesin-1 motor would either dissociate from MT with about 70% probability or continue to move with about 30% probability. Based on these experimental data, the equation for the run length of the kinesin-1 motor in the presence of stationary obstacles can be derived as follows. In the absence of the obstacle, the dissociation probability of the motor per step $P_d^{(0)} = \frac{d}{L_0}$. In the presence of the stationary obstacles, on average, the dissociation probability of the motor per step, which is caused solely by the obstacles, can be calculated by $P_d^{(0)} = \frac{0.7}{(R-1)}$, where it is implicitly assumed that the stationary obstacles are uniformly distributed on the MT filament and *R* is the ratio of tubulin number to obstacle number. Thus, in the presence of the stationary obstacles, the total dissociation probability of the motor per step can be calculated by $P_d^{(0)} + P_d^{(R)}$. The average run length of the motor can then be written as $L = \frac{d}{(P_d^{(0)} + P_d^{(R)})}$. With the above expressions for $P_d^{(0)}$ and $P_d^{(R)}$, *L* can be rewritten as

$$L = \frac{dL_0(R-1)}{d(R-1) + 0.7L_0}. \quad (17)$$

It should be mentioned that Equation (17) was derived without reference to any model for the kinesin motor and was derived based solely on the available experimental data[54].

As mentioned in Section 3, the experimental data of McVicker et al.[29] showed the motor's run length $L_0 \approx 1.31$μm with paclitaxel-stabilized MTs and $L_0 \approx 1.32$μm under the condition with glycerol/DMSO in the absence of tau. With $L_0 = 1.31$μm and using Equation (17), the calculated results of L/L_0 versus *R* are shown in Figure 7 (line), where for comparison we also show the corresponding experimental data for 3RS-tau (red dots) and for 4RL-tau (blue squares) under the condition with glycerol/DMSO[29]. It is seen that the theoretical results deviate significantly from the experimental data. From Figure 7 it is seen that at $R=5$, we have $L = 0.0337L_0 = 0.044$μm, which is more than 14-fold smaller than the experimental data of $L = 0.62$μm for 3RS-tau and $L = 0.84$μm for 4RL-tau at a 1:5 Tau/tubulin ratio with paclitaxel-stabilized MTs[29]. Even assuming that every

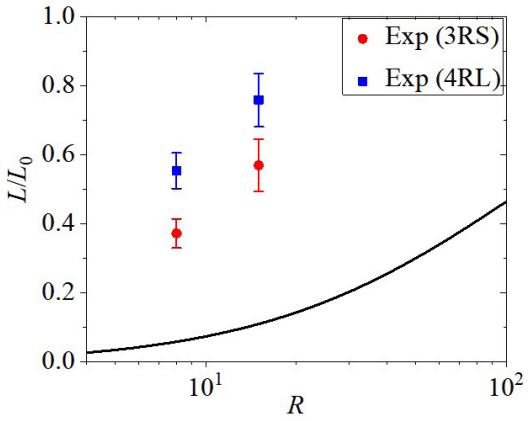

Figure 7. Dependence of the Run Length of the Kinesin Motor On Tubulin/Tau Ratio, *R*, for Stationary Tau. Line represents theoretical results with Equation (17). Red dots and blue squares are experimental data from McVicker et al.[29] measured under the condition with glycerol/DMSO.

10 tau molecules assembly into a cohesive envelope or island, which is approximately equivalent to R - 1=40 at a 1:5 tau/tubulin ratio, from Equation (17) and with L_0=1.31μm we obtain L=0.34μm, which is still evidently smaller than the experimental data of L=0.62m for 3RS-tau and L=0.84μm for 4RL-tau. To be consistent with L=0.62μm for 3RS-tau and L=0.84μm for 4RL-tau at a 1:5 tau/tubulin ratio, from Equation (17) and with L_0=1.31μm we obtain R-1=103 for 3RS-tau and R-1=205 for 4RL-tau, indicating that about 26 3RS-tau and 51 4RL-tau molecules assembly into a cohesive envelope or island. This implies that it is easier for 4RL-tau molecules to assembly into cohesive envelopes or islands than for 3RS-tau molecules, which is contrary to the prior experimental data showing that under the same condition the population in the static, interacting state for 4RL-tau molecules is smaller than that for 3RS-tau molecules[31]. All these results indicate that it is unreasonable to assume that tau molecules are stationary on the MT filament in the presence of the kinesin motors under the experimental condition of McVicker et al.[29].

Furthermore, consider the case (called case 2) that some tau molecules are in the static, interacting state while others are in the diffusing state. Similar to the above studies for the case (called case 1) that all tau molecules are in the static, interacting state, it can be deduced that to be consistent with the experimental data showing that at a given tau/tubulin ratio the run length for 4RL-tau is larger than that for 3RS-tau[29], for case 2 it is also required that the number of 4RL-tau molecules that assembly into a cohesive envelope or island is larger than that of 3RS-tau molecules. This is also contrary to the prior experimental data showing that under the same condition the population of 4RL-tau molecules in the static, interacting state is smaller than that of 3RS-tau molecules[31]. Thus, it is also unreasonable to assume that in the presence of the kinesin motors some tau molecules are in the static, interacting state while others are in the diffusing state under the experimental condition of McVicker et al.[29].

4.3 Effect of Occupancy Probability of Rear Tubulin by Tau on Dynamics of Kinesin Motor

In Section 2.3 and Section 3, it is approximately considered that at the INT state of Figure 1C, the probability of the front tubulin adjacent to the MT-bound head and that of the rear tubulin adjacent to the MT-bound head being occupied by a tau have the same form of P_O=1/R. This approximation is based on the consideration that during the period (called Period INT) after the trailing head detaches from the rear tubulin and before the large change in the conformation of the MT-bound ATP-head together with the reduction of the affinity between the two heads take place, either the event of a tau detaching from the adjacent MTs and then binding to the rear tubulin can occur or the event of a tau diffusing from the adjacent tubulins to the rear tubulin can occur. Thus, during Period INT the distribution of tau molecules on MTs can reach equilibrium.

In fact, when the stepping rate of tau, k_{tau}, along MT filament is very small, from the adjacent tubulins a tau has a small probability to diffuse to the rear tubulin during Period INT. Thus, the occupancy probability of the rear tubulin would be smaller than P_{OB}=1/R. Now, consider the limiting case, where no event of a tau detaching from MTs and then binding to the rear tubulin can occur during Period INT. This limiting case can give the following results. When k_{tau}=0, the occupancy probability P_{OB} approaches zero. When k_{tau} is very large, the distribution of tau molecules on the MT filament would equilibrate and thus P_{OB} would become equal to 1/R. When k_{tau} has a value larger than 0, the dependence of P_{OB} on k_{tau} should approximately have the form of $P_{OB}=(1/R)\exp(-a/k_{tau})$, where a is a constant. It is expected that a should be on the order of the stepping rate $k^{(+)}$ of the motor. Thus, the probability of the front tubulin being occupied, P_{OF}, and that of the rear tubulin being occupied, P_{OB}, by tau can be approximately written as

$$P_{OF}=\frac{1}{R}, \quad (18)$$

$$P_{OB}=\frac{1}{R}exp\left(-\frac{k^{(+)}}{k_{tau}}\right). \quad (19)$$

Then, from Equations (5)-(11) it is noted that after the reduction of the affinity between the two heads (Figure 1C), the occurrence probability of Period I, $P_{I1}^{(tau)}$, and the increase in the probability of the detached head binding to the rear tubulin in the presence of tau relative to that in the absence of tau, $P_{rear1}^{(tau)}$, can be rewritten as

$$P_{I1}^{(tau)}=P_{OF}-P_{OF}(1-P_{OB})\left(\frac{k_{tau}}{k_{tau}+\frac{1}{t_b}}\frac{k_{tau}}{k_{tau}+k^{(+)}}+\frac{\frac{1}{t_b}}{k_{tau}+\frac{1}{t_b}}\frac{\frac{1}{t_b}}{\frac{1}{t_b}+k^{(+)}}\right)$$
$$-P_{OF}P_{OB}\left[\frac{k_{tau}}{k_{tau}+\frac{1}{\left(t_b+\frac{1}{k_{tau}}\right)}}\frac{k_{tau}}{k_{tau}+k^{(+)}}+\frac{\frac{1}{\left(t_b+\frac{1}{k_{tau}}\right)}}{k_{tau}+\frac{1}{\left(t_b+\frac{1}{k_{tau}}\right)}}\frac{\frac{1}{\left(t_b+\frac{1}{k_{tau}}\right)}}{\frac{1}{\left(t_b+\frac{1}{k_{tau}}\right)}+k^{(+)}}\right], \quad (20)$$

$$P_{rear1}^{(tau)}=P_{OF}(1-P_{OB})\frac{\frac{1}{t_b}}{k_{tau}+\frac{1}{t_b}}\frac{\frac{1}{t_b}}{\frac{1}{t_b}+k^{(+)}}+P_{OF}P_{OB}\frac{\frac{1}{\left(t_b+\frac{1}{k_{tau}}\right)}}{k_{tau}+\frac{1}{\left(t_b+\frac{1}{k_{tau}}\right)}}\frac{\frac{1}{\left(t_b+\frac{1}{k_{tau}}\right)}}{\frac{1}{\left(t_b+\frac{1}{k_{tau}}\right)}+k^{(+)}}. \quad (21)$$

Similar to Equations (14) and (16), the ratios v/v_0 and L/L_0 can be written as

$$\frac{v}{v_0}=\frac{1}{1+P_{\text{rear1}}^{(\text{tau})}}, \quad (22)$$

$$\frac{L}{L_0}=\frac{1}{\left(1+P_{\text{rear1}}^{(\text{tau})}\right)\left(1+\frac{k^{(+)}P_{\text{l1}}^{(\text{tau})}}{\varepsilon_0}\right)}. \quad (23)$$

Using Equations (18)-(23), namely with P_{OF} and P_{OB} described by Equations (18) and (19), the calculated results of v/v_0 and L/L_0 versus D for R=5 are shown in Figure S5A and B, respectively, where for comparison the corresponding results calculated using Equations (4)-(16), namely with P_{OF}=P_{OB}=1/R, are also shown. The results of $\Delta(v/v_0)$ and $\Delta(L/L_0)$ versus D for R=5 are shown in Figure S5C and D, respectively, where $\Delta(v/v_0)$ and $\Delta(L/L_0)$ are the differences of v/v_0 and L/L_0 calculated with P_{OF} and P_{OB} described by Equations (18) and (19) relative to those calculated with P_{OF}=P_{OB}=1/R. From Figure S5, it is seen that at D≥0.05μm^2/s, both $\Delta(v/v_0)$ and $\Delta(L/L_0)$ calculated with P_{OF} and P_{OB} described by Equations (18) and (19) are almost identical to those calculated with P_{OF}=P_{OB}=1/R. At D<0.05μm^2/s, both $|\Delta(v/v_0)|$ and $|\Delta(L/L_0)|$ increase with the decrease of D.

To compare the theoretical results obtained using P_{OF} and P_{OB} described by Equations (18) and (19) with the available experimental data of McVicker et al.[29], in Figures S6-S8 (see Supplementary Materials) we show the results of v/v_0 and L/L_0 versus D for R=5, versus R for D=0.01μm^2/s and versus R for D=0.1μm^2/s, respectively, calculated using P_{OF} and P_{OB} described by Equations (18) and (19). Figures S6-S8 correspond respectively to Figures 3, 5 and 6, respectively. From Figures S6-S8, it is seen that with P_{OF} and P_{OB} described by Equations (18) and (19) the theoretical results are also in good agreement with the available experimental data[29].

Considering that during Period INT both the event that a tau detaches from MTs and then binds to the rear tubulin can occur and the event that a tau diffuses from the adjacent tubulins to the rear tubulin can occur, the occupancy probability of the rear tubulin should be in between P_{OB} described by Equation (19) and $P_{\text{OB}}=\frac{1}{R}$. Therefore, the results for v/v_0 and L/L_0 should be in between those calculated with $P_{\text{OF}}=P_{\text{OB}}=\frac{1}{R}$, as shown in Figures 3-6, and those calculated with P_{OF} and P_{OB} described by Equations (18) and (19), as shown in Figures S5-S8. As the former event makes the main contribution to the occupancy of the rear tubulin, the results for v/v_0 and L/L_0 should be more closer to those calculated with $P_{\text{OF}}=P_{\text{OB}}=\frac{1}{R}$, as shown in Figures 3-6.

4.4 Comparisons of The Theoretical Results with Published Experimental Data

As shown in Results section, the theoretical results are in agreement with the published experimental data of McVicker et al.[29] about the effect of tau on kinesin-1 motility, under the condition that in the presence of kinesin motors on MT the nearby tau proteins are in the diffusive state and the static tau proteins can transition into diffusive ones. Under the condition, tau only has a slight effect on the velocity of the kinesin-1 motor but can have a large effect on the inhibition of the run length. The long run length can be achieved with the large diffusion constant of tau.

Other published experimental data showed that under some conditions, where the presence of kinesin motors cannot induce the tau proteins assembled in the static cohesive envelopes or islands to transition into diffusive ones[43,53,55], tau proteins have different effects on the kinesin-1 motility. For example, while a kinesin-1 motor can move processively outside the boundary of the tau island, when reaching the island boundary the motor dissociates rapidly[55], similar to the case of kinesin-1 motor encountering a stationary obstacle[54,55]. The kinesin-1 motor can land within the tau island but the kinesin-1 landing within the island cannot move processively[55]. Under these conditions, the study presented in this work is not applicable. The effect of the static tau islands on the kinesin motility and how the kinesin-based long-distance axonal transport can be achieved in the presence of the static tau islands will be studied theoretically in future.

5 CONCLUSION

The effect of the diffusive tau on the dynamics of the kinesin motor is studied theoretically. With no adjustable parameter, the theoretical results are in agreement with the available experimental data about the velocity and run length of the motor moving on paclitaxel-stabilized MTs at a 1:5 tau/tubulin ratio. With only one adjustable parameter, the diffusion constant of tau, the theoretical results reproduce the available experimental data about the dependence of velocity and run length of the kinesin moving on MTs treated with glycerol/DMSO upon tubulin/tau ratio for different isoforms of tau.

The study shows that either the variation of the tau concentration or variation of the diffusion constant of tau can regulate the kinesin motility, thus regulating the long-distance axonal transport by the kinesin. Even with a large tau/tubulin ratio, tau has a slight effect on the velocity of the kinesin. By contrast, with a large tau/tubulin ratio, tau has a large effect on the run length of the kinesin and the run length depends sensitively on the diffusion constant of tau, with the run length increasing greatly with the increase of the diffusion constant and at the large diffusion constant the run length becoming leveled off to the one in the absence of tau. As failure of the long-distance axonal transport can lead to the neuronal disease, our results thus imply that

the capability of tau diffusing on MT with a large diffusion constant is helpful to the neuronal health.

Acknowledgements

This work was supported by the National Natural Science Foundation of China (No. 11775301).

Conflicts of Interest

There is no conflict of interest.

Data Availability

All data generated or analyzed during this study are included in this published article and its supplementary information files.

Author Contribution

Xie P was responsible for all the work on the article.

Abbreviation List

ADP, Adenosine diphosphate
ATP, Adenosine triphosphate
INT, Intermediate
MAP, Microtubule-associated protein
MT, Microtubule
NBP, Nucleotide-binding pocket
NL, Neck linker
Pi, Phosphate
3RS, 3-repeat short isoform
4RL, 4-repeat long isoform

References

[1] Vale RD. The molecular motor toolbox for intracellular transport. *Cell,* 2003; 112: 467-480.[DOI]

[2] Hirokawa N, Noda Y, Tanaka Y et al. Kinesin superfamily motor proteins and intracellular transport. *Nature Rev Mol Cell Bio,* 2009; 10: 682-696.[DOI]

[3] Howard J. The movement of kinesin along microtubules. *Annu Rev Physiol,* 1996; 58: 703-729.[DOI]

[4] Hirokawa N. Kinesin and dynein superfamily proteins and the mechanism of organelle transport. *Science,* 1998; 279: 519-526.[DOI]

[5] Holzbaur EL, Goldman YE. Coordination of molecular motors: from in vitro assays to intracellular dynamics. *Curr Opin Cell Biol,* 2010; 22: 4-13.[DOI]

[6] Kozielski F, Sack S, Marx A et al. The Crystal Structure of Dimeric Kinesin and Implications for Microtubule-Dependent Motility. *Cell,* 1997; 91: 985-994.[DOI]

[7] Asbury CL. Kinesin: world's tiniest biped. *Curr Opin Cell Biol,* 2005; 17: 89-97.[DOI]

[8] Block SM. Kinesin motor mechanics: binding, stepping, tracking, gating, and limping. *Biophys J,* 2007; 92: 2986-2995.[DOI]

[9] Cross RA. Mechanochemistry of the kinesin-1 ATPase. *Biopolymers,* 2016;105: 476-482.[DOI]

[10] Visscher K, Schnitzer MJ, Block SM. Single Kinesin Molecules Studied with a Molecular Force Clamp. *Nature,* 1999; 400: 184-189.[DOI]

[11] Coppin CM, Pierce DW, Hsu L et al. The load dependence of kinesin's mechanical cycle. *PNAS;* 1997; 94: 8539-8544.[DOI]

[12] Nishiyama M, Higuchi H, Yanagida T. Chemomechanical Coupling of the Forward and Backward Steps of Single Kinesin Molecules. *Nature Cell Biol,* 2002; 4: 790-797.[DOI]

[13] Taniguchi Y, Nishiyama M, Ishii Y et al. Entropy rectifies the Brownian steps of kinesin. *Nature Chem Biol,* 2005; 1: 342-347.[DOI]

[14] Hyeon C, Onuchic JN. Internal strain regulates the nucleotide binding site of the kinesin leading head. *PNAS,* 2007; 104: 2175-2180.[DOI]

[15] Xie P. Insight into the chemomechanical coupling mechanism of kinesin molecular motors. *Commun Theor Phys,* 2021; 73: 057601.[DOI]

[16] Mugnai ML, Hyeon C, Hinczewski M et al. Theoretical perspectives on biological machines. *Rev Mod Phys,* 2020; 92: 025001.[DOI]

[17] Cleveland DW, Hwo SY, Kirschner MW. Physical and chemical properties of purified Tau factor and the role of Tau in microtubule assembly. *J Mol Biol,* 1977; 116: 227-247.[DOI]

[18] Drubin DG, Kirschner MW. Tau protein function in living cells. *J Cell Biol,* 1986; 103: 2739-2746.[DOI]

[19] Bunker JM, Wilson L, Jordan MA et al. Modulation of microtubule dynamics by tau in living cells: implications for development and neurodegeneration. *Mol Biol Cell,* 2004; 15: 2720-2728.[DOI]

[20] Stamer K, Vogel R, Thies E et al. Tau blocks traffic of organelles, neurofilaments, and APP vesicles in neurons and enhances oxidative stress. *J Cell Biol,* 2002; 156: 1051-1063.[DOI]

[21] Seitz A, Kojima H, Oiwa K et al. Single-molecule investigation of the interference between kinesin, Tau and MAP2c. *EMBO J,* 2002; 21: 4896-4905.[DOI]

[22] Vershinin M, Carter BC, Razafsky DS et al. Multiple-motor based transport and its regulation by Tau. *PNAS,* 2007; 104: 87-92.[DOI]

[23] Dixit R, Ross JL, Goldman YE et al. Differential Regulation of Dynein and Kinesin Motor Proteins by Tau. *Science,* 2008; 319: 1086-1089.[DOI]

[24] Stoothoff W, Jones PB, Spires-Jones TL et al. Differential effect of three-repeat and four-repeat tau on mitochondrial axonal transport. *J Neurochem,* 2009; 111: 417-427.[DOI]

[25] Stamer K, Vogel R, Thies E et al. Tau blocks traffic of organelles, neurofilaments, and APP vesicles in neurons and enhances oxidative stress. *J Cell Biol,* 2002; 156: 1051-1063.[DOI]

[26] Li Q, Ferrare JT, Silver J et al. Cholesterol in the cargo membrane amplifies tau inhibition of kinesin-1-based transport. *PNAS,* 2023; 120: e2212507120.[DOI]

[27] Garcia ML, Cleveland DW. Going new places using an old MAP: tau, microtubules and human neurodegenerative disease. *Curr Opin Cell Biol,* 2001; 13: 41-48.[DOI]

[28] Goedert M, Spillantini MG, Jakes R et al. Multiple isoforms of human microtubule-associated protein tau: sequences and localization in neurofibrillary tangles of Alzheimer's disease. *Neuron,* 1989; 3: 519-526.[DOI]

[29] McVicker DP, Chrin LR, Berger CL. The Nucleotide-binding State of Microtubules Modulates Kinesin Processivity and the Ability of Tau to Inhibit Kinesin-mediated Transport. *J Biol Chem,* 2011; 286: 42873-42880.[DOI]

[30] Hinrichs MH, Jalal A, Brenner B et al. Tau Protein Diffuses along the Microtubule Lattice. *J Biol Chem,* 2012; 287: 38559-38568.[DOI]

[31] McVicker DP, Hoeprich GJ, Thompson AR et al. Tau interconverts between diffusive and stable populations on the microtubule surface in an isoform and lattice specific manner. *Cytoskeleton,* 2014; 71: 184-194.[DOI]

[32] Nam W, Epureanu BI. Dynamic model for kinesin-mediated long-range transport and its local traffic jam caused by tau proteins. *Phys Rev E,* 2017; 95: 012405.[DOI]

[33] Xie P. Theoretical analysis of dynamics of kinesin molecular motors. *ACS Omega,* 2020; 5: 5721-5730.[DOI]

[34] Xie P. Determinant factors for residence time of kinesin motors at

microtubule ends. *J Biol Phys,* 2023; 49: 77-93.[DOI]

[35] Raym S, Meyhoferm E, Milligan RA et al. Kinesin follows the microtubule's protofilament axis. *J Cell Biol,* 1993; 121: 1083-1093.[DOI]

[36] Santarella RA, Skiniotis G, Goldie KN et al. Surface-decoration of microtubules by human Tau. *J Mol Biol,* 2004; 339: 539-553.[DOI]

[37] Ferro LS, Fang Q, Eshun-Wilson L et al. Structural and functional insight into regulation of kinesin-1 by microtubule-associated protein MAP7. *Science,* 2022; 375: 326-331.[DOI]

[38] Xie P. Modeling study of the dynamics of kinesin-14 molecular motors. *J Phys Chem B,* 2022; 126: 8720-8734.[DOI]

[39] Guo S-K, Wang P-Y, Xie P. A model of processive movement of dimeric kinesin. *J Theor Biol,* 2017; 414: 62-75.[DOI]

[40] Moyer ML, Gilbert SP, Johnson KA. Pathway of ATP hydrolysis by monomeric and dimeric kinesin. *Biochemistry,* 1998; 37: 800-813.[DOI]

[41] Andreasson JOL, Milic B, Chen G-Y et al. Examining kinesin processivity within a general gating framework. *eLife,* 2015; 4: e07403.[DOI]

[42] Castle BT, McKibben KM, Rhoades E et al. Tau avoids the GTP cap at growing microtubule plus-ends. *iScience,* 2020; 23: 101782.[DOI]

[43] Tan R, Lam AJ, Tan T., Han J, Nowakowski DW, Vershinin M, Simo S, Ori-McKenney KM, McKenney RJ. Microtubules gate tau condensation to spatially regulate microtubule functions. *Nature Cell Biol,* 2019; 21: 1078-1085.[DOI]

[44] Verhey KJ, Ohi R. Causes, costs and consequences of kinesin motors communicating through the microtubule lattice. *J Cell Sci,* 2023; 136: jcs260735.[DOI]

[45] Shi XX, Wang PY, Chen H et al. Studies of conformational changes of tubulin induced by interaction with kinesin using atomistic molecular dynamics simulations. *Int J Mol Sci,* 2021; 22: 6709.[DOI]

[46] Shima T, Morikawa M, Kaneshiro J et al. Kinesin binding-triggered conformation switching of microtubules contributes to polarized transport. *J Cell Biol,* 2018; 217: 4164-4183.[DOI]

[47] Peet DR, Burroughs NJ, Cross RA. Kinesin expands and stabilizes the GDP-microtubule lattice. *Nature Nanotechnol,* 2018; 13: 386-391.[DOI]

[48] Vilfan A, Frey E, Schwabl F et al. Dynamics and cooperativity of microtubule decoration by the motor protein kinesin. *J Mol Biol,* 2001; 312: 1011-1026.[DOI]

[49] Muto E, Sakai H, Kaseda K. Long-range cooperative binding of kinesin to a microtubule in the presence of ATP. *J Cell Biol,* 2005; 168: 691-696.[DOI]

[50] Roos WH, Campas O, Montel F et al. Dynamic kinesin-1 clustering on microtubules due to mutually attractive interactions. *Phys Biol,* 2008; 5: 046004.[DOI]

[51] Wijeratne SS, Fiorenza SA, Neary AE et al. Motor guidance by long-range communication on the microtubule highway. *PNAS,* 2022; 119: e2120193119.[DOI]

[52] Xie P. A model for cooperativity of kinesin-4 motors by communicating through the microtubule track. *Chem Phys,* 2024; 581: 112274.[DOI]

[53] Siahaan V, Tan R, Humhalova T et al. Microtubule lattice spacing governs cohesive envelope formation of tau family proteins. *Nature Chem Biol,* 2022; 18: 1224-1235.[DOI]

[54] Schneider R, Korten T, Walter WJ et al. Kinesin-1 motors can circumvent permanent roadblocks by side-shifting to neighboring protofilaments. *Biophys J,* 2015; 108: 2249-2257.[DOI]

[55] Siahaan V, Krattenmacher J, Hyman AA et al. Kinetically distinct phases of tau on microtubules regulate kinesin motors and severing enzymes. *Nature Cell Biol,* 2019; 21: 1086-1092.[DOI]